

Estimations of the cosmological parameters from the observational variation of the fine structure constant

Zhong-Xu Zhai,^{1,2} Xian-Ming Liu,^{3,2} Zhi-Song Zhang,⁴ and Tong-Jie Zhang^{1,5,*}

¹*Department of Astronomy, Beijing Normal University, Beijing, 100875, China*

²*Department of Physics, Institute of Theoretical Physics,
Beijing Normal University, Beijing, 100875, China*

³*Department of Physics, Hubei University for Nationalities, Enshi Hubei, 445000, China*

⁴*Department of Aerospace Engineering, School of Astronautics,
Harbin Institute of Technology (HIT), Harbin Heilongjiang, 150001, China*

⁵*Center for High Energy Physics, Peking University, Beijing, 100871, China*

We present the constraints on the Quintessence scalar field model from the observational data of the variation of the fine structure constant obtained from Keck and VLT telescopes. Within the theoretical frame proposed by Bekenstein[12], the constraints on the parameters of the Quintessence scalar field model are obtained. By the consideration of the prior of Ω_{m0} as WMAP 7 suggests [29], we obtain various results of the different samples. Based on these results, we also calculate the probability density function of the coupling constant ζ . The best-fit values show a consistent relationship between ζ and the different experimental results. In our work, we test two different potential models, namely, the inverse power law potential and the exponential potential. The results show that both the large value of the parameters in the potential and the strong coupling can cause the variation of fine structure constant.

PACS numbers: 98.54.Aj,98.80.Es,95.36.+x

I. INTRODUCTION

Fundamental constants play important roles in physics and its mathematical laws. By the information they contain, one can describe the phenomena of nature and obtain a better understanding of the real world [1]. However, one may suspect whether the constants are real "constants", i.e. do the constants vary with time or space? This question was probably first asked by Dirac with his famous "Large Numbers Hypothesis"(LNH) [2, 3]. Thereafter, several works have been done to investigate the underground principle, including researches of the variations of the constants and the measurements of their precise values. We refer the readers to the reviews [4–11] for more comprehensive discussions.

In order to unify the fundamental interactions theoretically, different theories are proposed including string derived field theories, brane-world theories, Kaluza-Klein theories which are based on the introduction of the extra dimensions. Among the constants, the fine structure constant α which measures the strength of the electromagnetic interaction attracts a lot of attention. In 1982, Bekenstein proposed a different theoretical framework to study α variability where a linear coupling between a scalar field and the electromagnetic field was introduced [12]. This theory satisfies the general conditions: covariance, gauge invariance, causality, and time-reversal invariance of electromagnetism. Later on, this proposal was generalized and improved by [13]. So far we have several different theories which can describe the

time evolution of the gauge coupling constants. However, whether the theoretical predictions can provide consistent results with the experimental ones should be asked. In this paper, we limit ourselves to study the Bekenstein model and the time-evolving behavior of the fine structure constant. The experiments which imply a time-related α include the observation of the Oklo natural nuclear reactor [14, 15], Big Bang Nucleosynthesis(BBN)[16–18], Cosmic Microwave Background (CMB) measurements [16, 17, 19–21], absorption spectra of distant Quasars(QSOs) [22–25], and so on. These observations give different measurements of α at different cosmological evolution periods. Among these observations, QSO absorption lines provide a powerful probe of the variation of α and a large data sample. The methods studying this observation results include the *alkali doublet method* (AD), the *many-multiplet method* (MM), the *revised many-multiplet method* (RMM), and the *Single ion differential alpha measurement method* (SIDAM) [1]. Because the observation by MM gives the widest range of redshift ($0.22 < z < 4.2$) [23, 26], it may contain more information of the cosmological evolution than the others. Thus we will mainly focus on these measurement in the present work. More details about the observational data will be presented in Sec.III

On the other hand, since its discovery more than ten years ago, the cosmic accelerated expansion has been demonstrated by the observations of type Ia supernovae and this phenomena is accepted widely [27–32]. In order to explain this amazing discovery, a great variety of attempts have been done including the introduction of dark energy and the modified gravity theories [33]. Among these proposals, the scalar field as a dynamical dark energy model was studied widely and deeply [34–

*Electronic address: tjzhang@bnu.edu.cn

36]. Therefore, the cosmological variation of α induced by coupling with the Quintessence, which is a typical scalar field dark energy, is worth studying in order to find if the QSO observations contain the information of the cosmic accelerated expansion. In other words, whether the QSO observations can give a consistent result with other cosmological probes, such as Type Ia Supernovae (SNe Ia), CMB, Baryon acoustic oscillation (BAO), Observational Hubble parameter Data (OHD) [37–39] and so forth, should be tested. Moreover, if the observation of QSO absorption lines provides consistent results with the ones listed above, can it be thought as an indirect proof of the existence of the scalar field (Quintessence)? This will be a very interesting question. In addition, we should notice that there is some difference between the QSO observations in [23, 25] and [22, 24]. The results analyzed by these two MM methods show an inconsistency of the time evolution of α . Thus what information of cosmological evolution these data contained respectively should be studied.

Following this direction, we constrain the cosmological parameters of the Quintessence dark energy model with the variational α data from the observation of the QSO absorption lines. One should note that there are several freedoms in choosing the form of the scalar field potential which plays an important role in the scalar field evolution. In our paper, we firstly focus on the inverse power-law potential $V(\phi) \propto \phi^{-n}$, where n is a nonnegative constant [40, 41]. This assumption has several advantages such as it can reduce to the standard Λ CDM case when $n = 0$ and contain the solutions which can alleviate the fine-tuning problem [42]. Recent researches of the mass scale of the inverse power law potential show that the field value at present is of order the Planck mass ($\phi_0 \sim M_P$) [33, 43, 44]. For comparison, we also consider another potential model $V(\phi) \propto e^{-\lambda\phi}$, where λ is a positive constant [41]. This model was first motivated by the anomaly of the dilatation symmetry in the particle physics and has the tracker solution at the late time [45, 46]. In this paper we just consider a spatially-flat Quintessence model.

Many previous works that constrain the parameters of the Quintessence dark energy model show that the universe is composed by about 30% nonrelativistic matter while the dark energy contributes nearly 70%. And the parameter n (of the inverse power law potential) and λ (of the exponential potential) which affects the evolution behavior of the scalar field directly both favor small values [36, 47, 48]. So we should ask to what extent are the constraints from QSO observations consistent with these results. The possibility of studying the fine structure constant under the dark energy models has been proposed from various aspects, including the reconstruction of the dark energy equation of state [49–51] or combined with other cosmological observations [52]. In this paper we will discuss the possibility of constraining the quintessence dark energy model with the direct measurements of the variation of fine structure constant.

Our paper is organized as follows. In Sec.II, we will present the basic formulas of the Quintessence- α model. The data used and the corresponding constraints are shown in Sec.III. The conclusion is presented in Sec.IV.

II. QUINTESSENCE AND THE ELECTROMAGNETIC COUPLINGS

We consider a spatially-flat FRW cosmology where the metric can be written as

$$ds^2 = -dt^2 + a(t)^2(dr^2 + r^2d\theta^2 + r^2\sin^2\theta d\varphi^2), \quad (1)$$

where a is the scale factor. Under this geometrical background, the evolution of the Quintessence scalar field ϕ is determined by the Friedmann equation and the Klein-Gordon equation

$$H^2 = \left(\frac{\dot{a}}{a}\right)^2 = \frac{8\pi}{3M_p^2} \sum \rho_i, \quad (2)$$

$$\ddot{\phi} + 3H\dot{\phi} + \frac{dV}{d\phi} = 0, \quad (3)$$

where M_p is the Planck mass, the overdot is the derivative with respect to the cosmic time t , ρ stands for the density and $i = m, \phi$ runs over the matter (including dark matter) and scalar components. The relevant equations of state are $\omega_m = 0$ for matter and $\omega_\phi = p_\phi/\rho_\phi$ for scalar field where

$$p_\phi = \frac{\dot{\phi}^2}{2} - V(\phi), \quad \rho_\phi = \frac{\dot{\phi}^2}{2} + V(\phi). \quad (4)$$

In our calculation, the function form of the potential are

$$\text{Model I} \quad V(\phi) = \kappa M_p^2 \phi^{-n}, \quad (5)$$

$$\text{Model II} \quad V(\phi) = V_0 e^{-\lambda\phi}, \quad (6)$$

where κ, V_0 are non-negative constants, n and λ are the parameter will be constrained by the data. These kinds of scalar field model was first studied by Peebles and Ratra in 1988 and further explored especially in explaining the dark energy problem[34, 36, 53–56](and references therein). By the definitions of the dimensionless parameters

$$\Omega_m = \frac{8\pi\rho_m}{3M_p^2 H^2} = \frac{\rho_m}{\rho_m + \rho_\phi}, \quad \Omega_\phi = \frac{8\pi\rho_\phi}{3M_p^2 H^2} = \frac{\rho_\phi}{\rho_m + \rho_\phi}, \quad (7)$$

the Friedmann Equation Eq.(2) can be rewritten in a simple form

$$\Omega_m + \Omega_\phi = 1. \quad (8)$$

So far our model is determined by only two parameters (Ω_{m0}, n) for Model I and (Ω_{m0}, λ) for Model II, where the subscript 0 stands for the present value. This parameter set is the key point that will be constrained by the observational data.

Considering an interaction between a Quintessence field ϕ and an electromagnetic field $F_{\mu\nu}$, we can write its Lagrangian density as

$$\mathcal{L}_F(\phi) = -\frac{1}{4}B_F(\phi)F_{\mu\nu}F^{\mu\nu}, \quad (9)$$

where $B_F(\phi)$ is the function that describes the coupling behavior. One should note that the addition of this interaction term does not affect the evolution of the quintessence scalar field. This is due to the fact that the statistical average of $F_{\mu\nu}F^{\mu\nu}$ over a current state of the universe is zero [57, 58]. Thus Eq.(3) is still applicable. The Lagrangian form Eq.(9) allows us to define a new "effective" fine structure constant

$$\alpha(\phi) = \frac{\alpha_0}{B_F(\phi)}, \quad (10)$$

where α_0 is the current value. By the use of this equation we can obtain a relative variation of α

$$\frac{\Delta\alpha}{\alpha} = \frac{\alpha(\phi) - \alpha_0}{\alpha_0} = \frac{1 - B_F(\phi)}{B_F(\phi)}. \quad (11)$$

Apparently, the evolution of α is directly affected by ϕ and the functional form $B_F(\phi)$. From the theoretical view, there are many choices in defining B_F which leads to different α behaviors. The authors of [58] give a detailed discussion about $B_F(\phi)$ which contains many different cases. In our paper, we will consider the simplest case which is a linear form and corresponds to the original Bekenstein proposal [12],

$$B_F(\phi) = 1 - \zeta(\phi - \phi_0), \quad (12)$$

where the constant ζ describes the strength of the coupling between the scalar field and the electromagnetic field. We will see that the parameter sets (Ω_{m0}, n, ζ) and $(\Omega_{m0}, \lambda, \zeta)$ completely describe the evolution behavior of the Quintessence- α Model I and Model II respectively.

III. THE OBSERVATIONAL QSO DATA AND CONSTRAINTS

A. the observational QSO data

The MM method as a generalization of the AD method was first proposed in [59]. It was first applied in [25] to analyze the distant QSO absorption lines observed by Keck which is located in Hawaii. Their result shows a variation of α in the redshift range of $0.6 < z < 1.6$. Later on, more QSO systems were observed and the data sample was enlarged. The updated results which are based on a statistical analysis including 143 absorption systems show that $\Delta\alpha/\alpha = (-0.57 \pm 0.11) \times 10^{-5}$ in the redshift range of $0.2 < z < 4.2$ [23]. We will use this data sample to test the Quintessence- α model. For convenience, we use "KWM143" as an abbreviation for this sample. Although there are some differences in analyzing the low- z

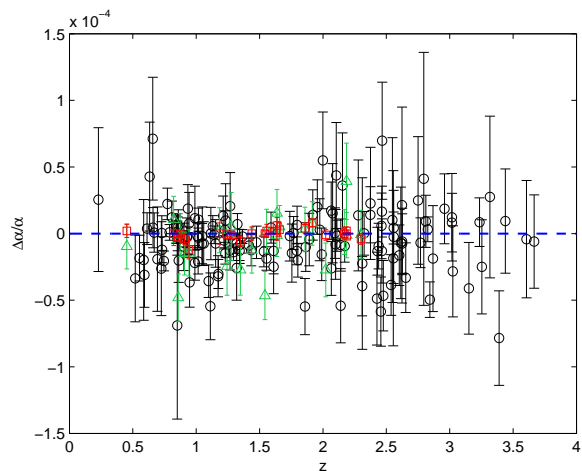


FIG. 1: The direct measurements of $\Delta\alpha/\alpha$ with respect to the redshift z : VCS23(square); VMW23(triangle); KMW128(circle). The dashed curve is the horizontal line indicating no variation.

and high- z absorption systems, we will combine the total 143 data to do the calculation and neglect the tiny discrepancies.

On the other hand, a further independent statistical study was completed in [22, 24] based on the observations of VLT. Their calculation favors a different result of $\Delta\alpha/\alpha = (-0.06 \pm 0.06) \times 10^{-5}$ which shows a nearly unchanged α in the redshift range of $0.4 < z < 2.3$. However, this analysis was challenged by [60] who used the same reduced data and got a result of $\Delta\alpha/\alpha = (-0.44 \pm 0.16) \times 10^{-5}$ in the same redshift range. However this result is not reliable because of its larger value of the reduced χ^2 in [60]. Therefore it is necessary to consider the additional scatter and the systematic error which derive the most conservative weighted mean result becomes $\Delta\alpha/\alpha = (-0.64 \pm 0.36) \times 10^{-5}$. This result also prefers a non-zero variation of the fine structure constant. Since then, this contradictory results were discussed several times by different research groups and the principles behind the observations were explored from many different aspects [61–75]. Recently, an intensive debate in literature was proposed by [76–78]. They propose that the observed spatial variation of α is really an artificial effect, resulting from the fact that Keck and VLT are located at different hemispheres. Therefore perhaps it is worth noticing to study the possibility of the spatial variation of α in the quintessence model, but the new physics may be taken into account. In our calculation, we will use these two different data samples independently and constrain the Quintessence- α model respectively. One of our goals is to explore the reasons that cause the above two different results, i.e. aiming at finding out whether the coupling strength or the cosmological evolution of quintessence leads to the discrepancy between them. In the following, we use "VCS23" and "VWM23" as abbreviations.

viations for these two samples. In TABLE.I and FIG.1, we recollect the direct measurements of $\Delta\alpha/\alpha$ from the works listed above.

From Eq.(11) and (12), we can see that the value of ζ effects the evolution of $\Delta\alpha/\alpha$ directly. From the tests of the equivalence principle the coupling is constrained to be $|\zeta| < 10^{-3}$ [79, 80]. Furthermore, Copeland et al. [57] used a simple estimation to obtain an approximate value of $\zeta \approx 10^{-5}$ which is under the assumption of inverse power law potential and the QSO observations. In our paper, we consider ζ as a free parameter to be constrained by the data and compare the results with the previous works such as the Equivalence Principle test [81–83] which shows that $|\zeta| < 5 \times 10^{-4}$.

B. Constraints with a prior of Ω_{m0}

In order to get the best-fit results of the parameters of the Quintessence- α model, we apply the χ^2 statistics to the observational QSO data

$$\chi^2(z; \Omega_{m0}, n; \zeta) = \sum_i \left(\frac{(\Delta\alpha/\alpha)_{th,i} - (\Delta\alpha/\alpha)_{obs,i}}{\sigma_i} \right)^2, \quad (13)$$

where the subscripts "th" and "obs" stand for the theoretically predicted value and observed ones respectively. In order to obtain the purely results, we do not take into account other experimental bounds as mentioned in Sec.I of our χ^2 calculation, but the comparisons of the single QSO constraints with other experiments are worth studying and are carried out in the later sections. For the purpose of reducing the unnecessary distractions arising from the intrinsic complexity of this scalar field model, it is convenient to set reasonable priors on some of the parameters.

As mentioned in the previous sections, one important discovery of the cosmology is the present accelerated expansion. This discovery indicates that the universe contains the so-called "dark energy" component much more than the ordinary matter, i.e. in our quintessence- α model, the parameter Ω_{m0} should occupy a relative smaller proportion. Therefore, we adopt a Gaussian distribution of $\Omega_{m0} = 0.275 \pm 0.016$ as WMAP 7 suggests [29] to be a prior to constrain the quintessence- α model. Thus the parameters which will be constrained are (n, ζ) for Model I and (λ, ζ) for Model II.

Our constraints results are shown in FIG.2-FIG.4. Generally speaking, for Model I, the best-fit values of the Quintessence- α model obtained from three data samples all favor a small value of n . This feature is consistent with most other cosmic probes which show that $n < 1.5$ [36]. This phenomena shows that the scalar field evolves slowly in the universe. And the value of n is smaller, the scalar field model is closer to the standard Λ CDM. Except that, the two contradictory samples VCS23 and VWM23 both indicate $n = 0.1$. The main differences between these constraints results are the big discrepancies

of the value of ζ . The value obtained by VWM23 is much larger than the other two samples, while the VCS23 gives the smallest one.

For Model II, the constraints show similar trends of the parameters. The best-fit value of λ obtained by KWM143 is apparently larger than the other two data samples. But the coupling constant ζ of VCS23 is larger than KWM143 which is different from Model I case.

Additionally, these results of two models are also consistent with the Equivalence Principle test. But we should note that the observations of the variations of fine structure constant can not give efficient constraint on the cosmological parameter n and λ . Therefore it is difficult to identify the current evolutionary state of the universe, i.e. the evolution of $\Delta\alpha/\alpha$ is not as sensitive to the cosmological parameters as to the coupling constant ζ . One more point worth noticing is that from our results, the variation of α can be caused by large value of n or λ , or the strong coupling constant ζ . This can be obtained from the comparisons of the constraints, it is shown that the different weighted values of VWM23 and VCS23 is attributed to the variance of ζ instead of cosmological parameters. However, the similar results of KWM23 and VWM23 do not give constrict consistent constraint, VWM23 gives smaller n and λ but larger ζ . Therefore, the goal of finding the reasons causing the variation of α is still vague. But we should emphasize that the above conclusions are not sure enough because of the insufficient constraints of n and λ even the 1σ confident regions are not perfectly obtained.

C. the probability density function of ζ

The previous constraints show a 2 dimensional distribution of the parameters (n, ζ) and (λ, ζ) . In order to compare the value of ζ with other tests, it is necessary to calculate the probability density function (PDF) of ζ by marginalizing the parameter n or λ . Our results are presented in FIG.5 to FIG.7.

Generally speaking, the results obtained are compatible with the Equivalence Principle test which is $|\zeta| < 5 \times 10^{-4}$. But the differences between these calculations are also significant. FIG.5 shows a apparent result that the best-fit value of ζ is nearly zero for both models. The small coupling constant indicates a case that the coupling between the electromagnetic field and the scalar field is so weak that the fine structure constant is nearly unchanged. While FIG.6 and FIG.7 show different results. Both of VWM23 and KWM143 give a similar value of ζ in each model. Their results are consistent with each other and favor a variation of α . It is noteworthy that the constraint from VWM23 is not as strict as KWM143 which may be attributed to the smaller size of this sample. Comparing two models, the best-fit values of ζ are larger in Model II than Model I, this implies that the coupling between the scalar field and electromagnetic field is stronger in the exponential potential than the inverse

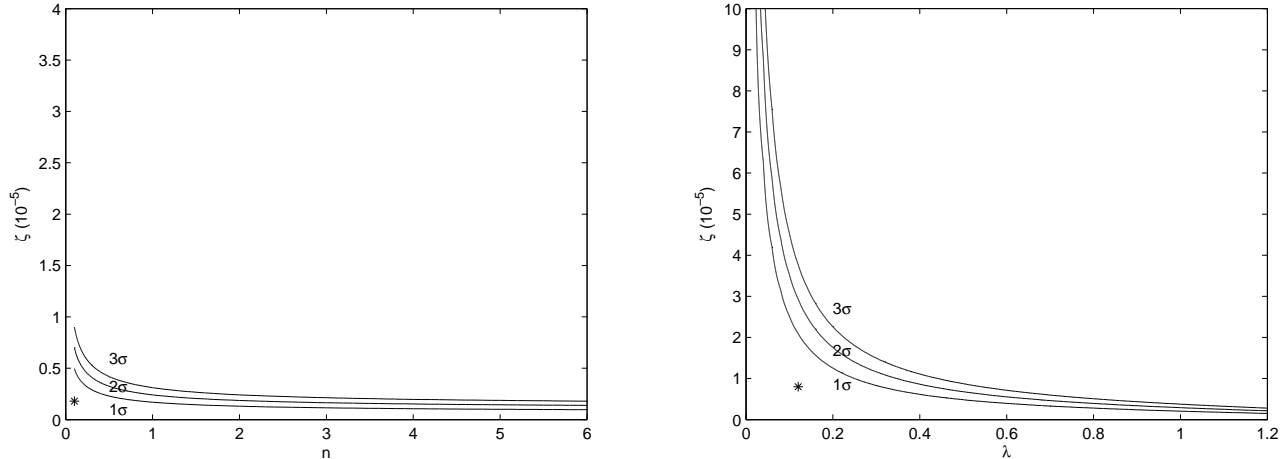


FIG. 2: *Left*(Model I): The confident regions of (n, ζ) obtained from VCS23 with a prior of Ω_m . The best-fit results which is indicated by the star are $(n, \zeta) = (0.1, 0.18 \times 10^{-5})$ with $\chi_{min}^2 = 27.7919$. *Right*(Model II): The confident regions of (λ, ζ) obtained from VCS23 with a prior of Ω_m . The best-fit results which is indicated by the star are $(\lambda, \zeta) = (0.12, 0.80 \times 10^{-5})$ with $\chi_{min}^2 = 27.6141$

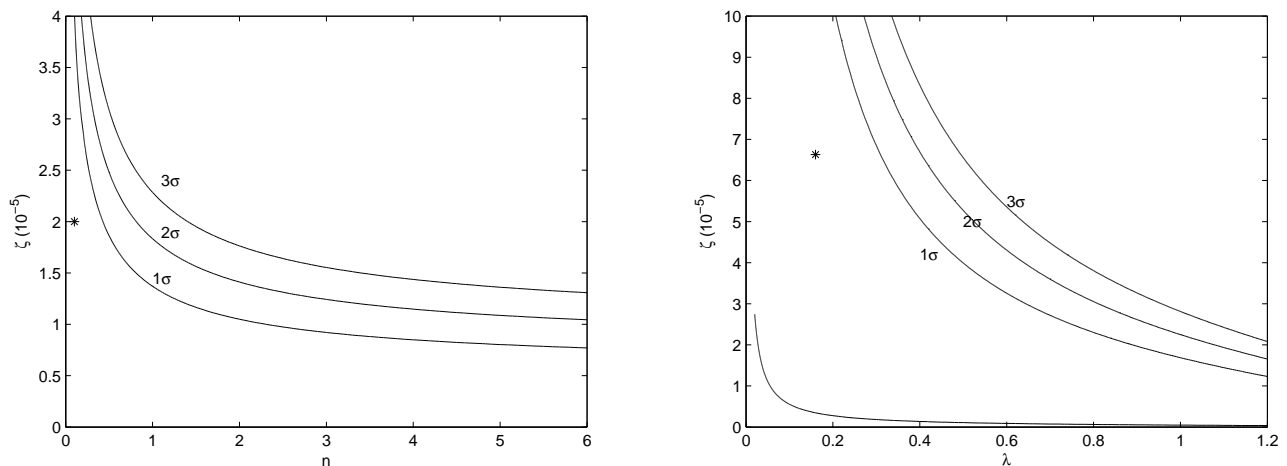


FIG. 3: *Left*(Model I): The confident regions of (n, ζ) obtained from VWM23 with a prior of Ω_m . The best-fit results which is indicated by the star are $(n, \zeta) = (0.1, 2.0 \times 10^{-5})$ with $\chi_{min}^2 = 29.2648$. *Right*(Model II): The confident regions of (λ, ζ) obtained from VWM23 with a prior of Ω_m . The best-fit results which is indicated by the star are $(\lambda, \zeta) = (0.16, 6.63 \times 10^{-5})$ with $\chi_{min}^2 = 28.8861$.

power law potential. Except that, we also notice that once compared with the results obtained in Sec.III B, an apparent discrepancy between the constraints of ζ from VWM23 FIG.3 and FIG.6 emerges. This result is understandable because the 2 dimensional constraints or the corresponding likelihood function is non-gaussian. This comes from the quality of the data or the non-linearity of the theoretical function.

D. comparison with other experiments

In this section, we consider the comparison of the QSO constraint results with other experiments. In order to obtain a clear impression, we plot the evolutions of the scalar field ϕ and $\Delta\alpha/\alpha$ with respect to redshift z in FIG.8 and FIG.9 (the top and middle panels). Firstly, we consider the Oklo natural reactor which provides a bound at 95% confident level,

$$-0.9 \times 10^{-7} < \frac{\Delta\alpha}{\alpha} < 1.2 \times 10^{-7} \quad (14)$$

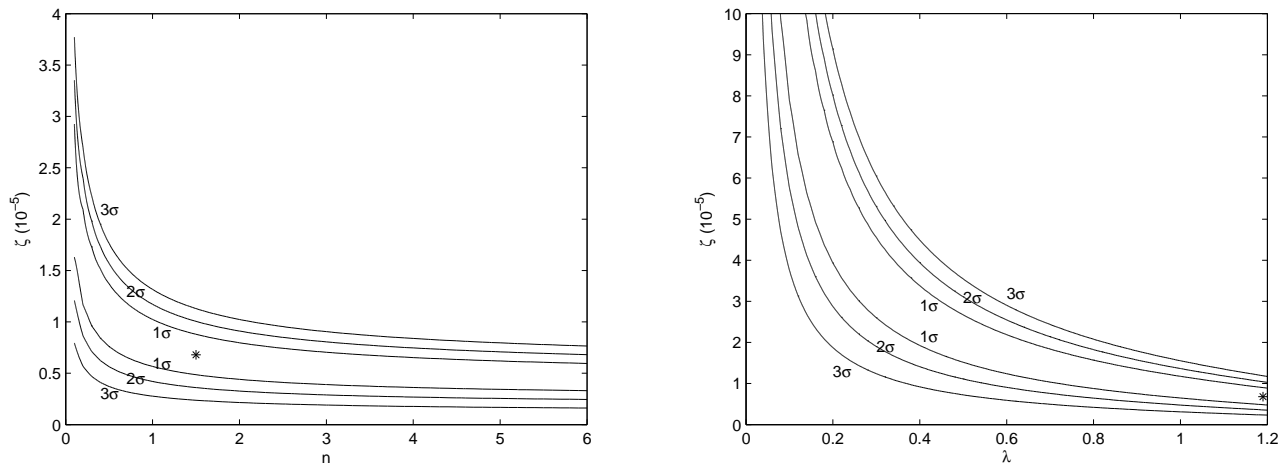


FIG. 4: *Left*(Model I): The confident regions of (n, ζ) obtained from KWM143 with a prior of Ω_m . The best-fit results which is indicated by the star are $(n, \zeta) = (1.5, 0.68 \times 10^{-5})$ with $\chi_{min}^2 = 149.5672$. *Right*(Model II): The confident regions of (λ, ζ) obtained from VWM23 with a prior of Ω_m . The best-fit results which is indicated by the star are $(\lambda, \zeta) = (1.2, 0.68 \times 10^{-5})$ with $\chi_{min}^2 = 149.9395$.

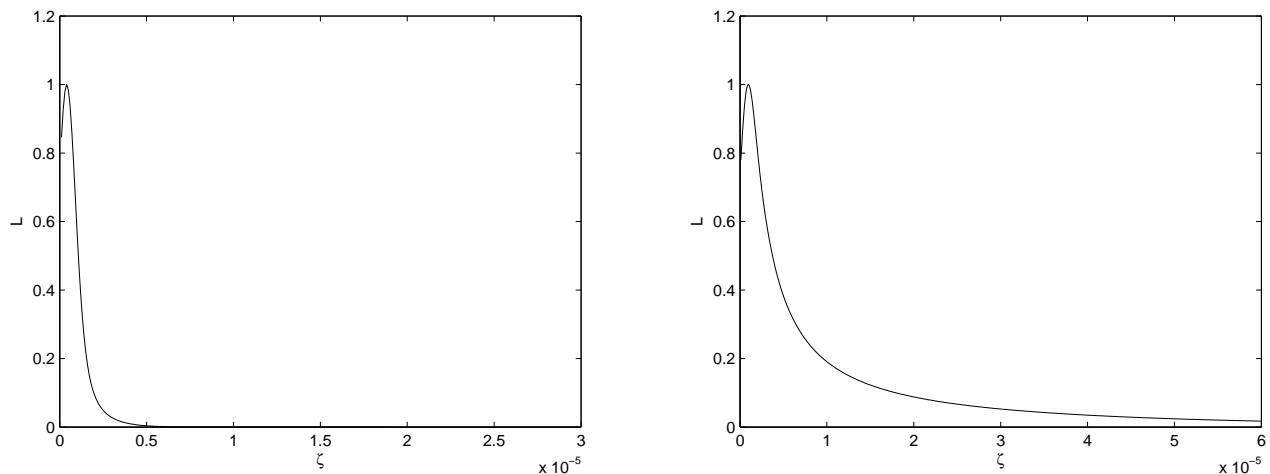


FIG. 5: *Left*(Model I): The PDF of ζ obtained from VCS23. The most probable point is located at $\zeta = 0.04 \times 10^{-5}$. *Right*(Model II): The PDF of ζ obtained from VCS23. The most probable point is located at $\zeta = 0.10 \times 10^{-5}$.

for $z = 0.14$ [14, 84, 85]. Except that, the estimates of the age of iron meteorites at $z = 0.45$ combined with a measurement of the Os/Re ratio resulting from the radioactive decay $^{187}\text{Re} \rightarrow ^{187}\text{Os}$ gives [15, 86, 87]

$$\frac{\Delta\alpha}{\alpha} = (-8 \pm 8) \times 10^{-7} \quad (15)$$

at 1σ and

$$-24 \times 10^{-7} < \frac{\Delta\alpha}{\alpha} < 8 \times 10^{-7} \quad (16)$$

at 2σ [88].

The results are presented in the bottom panels of FIG.8 and FIG.9. Compared with the QSO results, the Oklo

measurements and meteorites estimates both favor a unchange value of the fine structure constant, because they are consistent with VCS23 constraint except a tiny deviation of Model II bounded by the Oklo measurement. Compared with Oklo, the meteorites observations give a wider range of uncertainty, however, the VWM23 and KWM143 both violate this bound. Furthermore, the larger value of the slope of Model II at low redshift shows a more drastic deflection from the meteorites constraint.

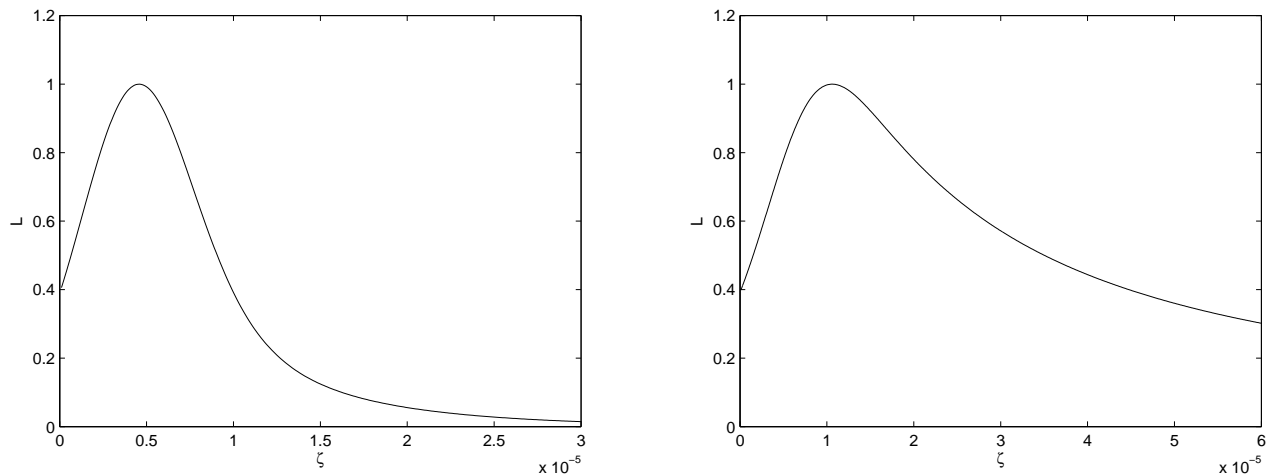


FIG. 6: *Left*(Model I): The PDF of ζ obtained from VWM23. The most probable point is located at $\zeta = 0.46 \times 10^{-5}$. *Right*(Model II): The PDF of ζ obtained from VWM23. The most probable point is located at $\zeta = 1.06 \times 10^{-5}$.

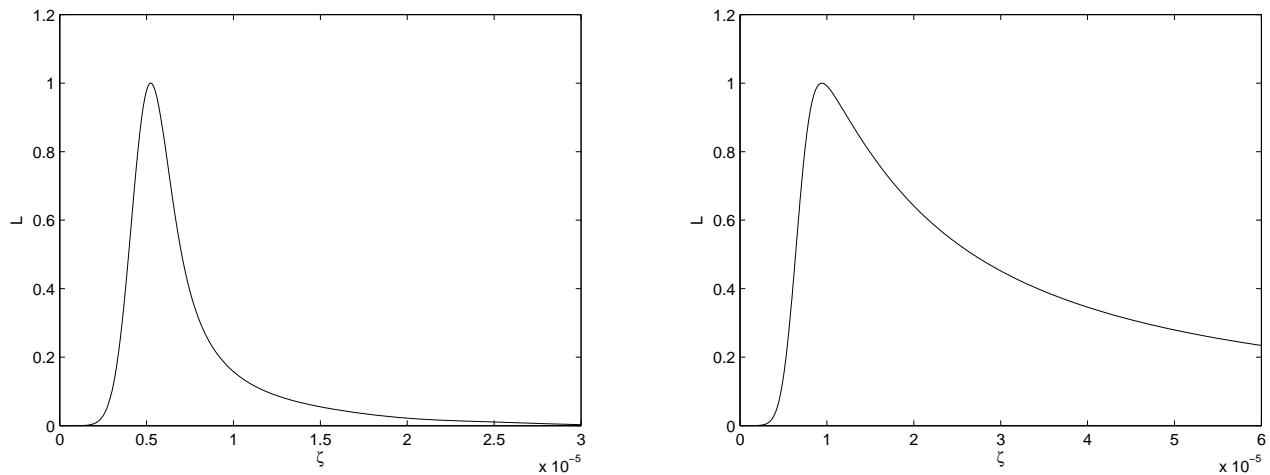


FIG. 7: *Left*(Model I): The PDF of ζ obtained from KWM143. The most probable point is located at $\zeta = 0.52 \times 10^{-5}$. *Right*(Model II): The PDF of ζ obtained from KWM143. The most probable point is located at $\zeta = 0.94 \times 10^{-5}$.

IV. DISCUSSIONS AND CONCLUSION

In the present paper, we present the constraints of the cosmological parameters on the Quintessence model by the measurements of the variation of fine structure constant α from distant QSOs. By the use of the Gaussian prior of Ω_{m0} , three data samples KWM143, VWM23, and VCS23 give apparent various constraints of the parameters. For both of the two potential models, VCS23 shows the smallest ζ which can be treated as an explanation of the results of [22] because the weak coupling derives a weak interaction with the electromagnetic field. This leads to an unchanging of α . On the other hand, VWM23 and KWM143 present a result that the values of ζ are larger especially the VWM23 one, while the constraints of n for Model I and λ for Model II are different. And

the strong coupling strength implies the possibility of a variation of α . In order to further study this problem, we marginalize the cosmological parameter n or λ and obtain the PDF of ζ . The results confirm our analysis that the VCS23 favors a nearly null result of ζ . Except that, the discrepancy between the VWM23 and KWM143 about ζ disappeared and provide consistent constraints of it. Combined the two models, we find that either a strong coupling or a large value of the cosmological parameters (here refers to n or λ) can lead to an apparent variation of α . Our results show that the difference between VWM23 and VCS23 is caused by the different coupling constant, while the similar results of VWM23 and KWM143 have different reasons. The former is attributed to a stronger coupling and the latter is caused by a different evolution of quintessence scalar field.

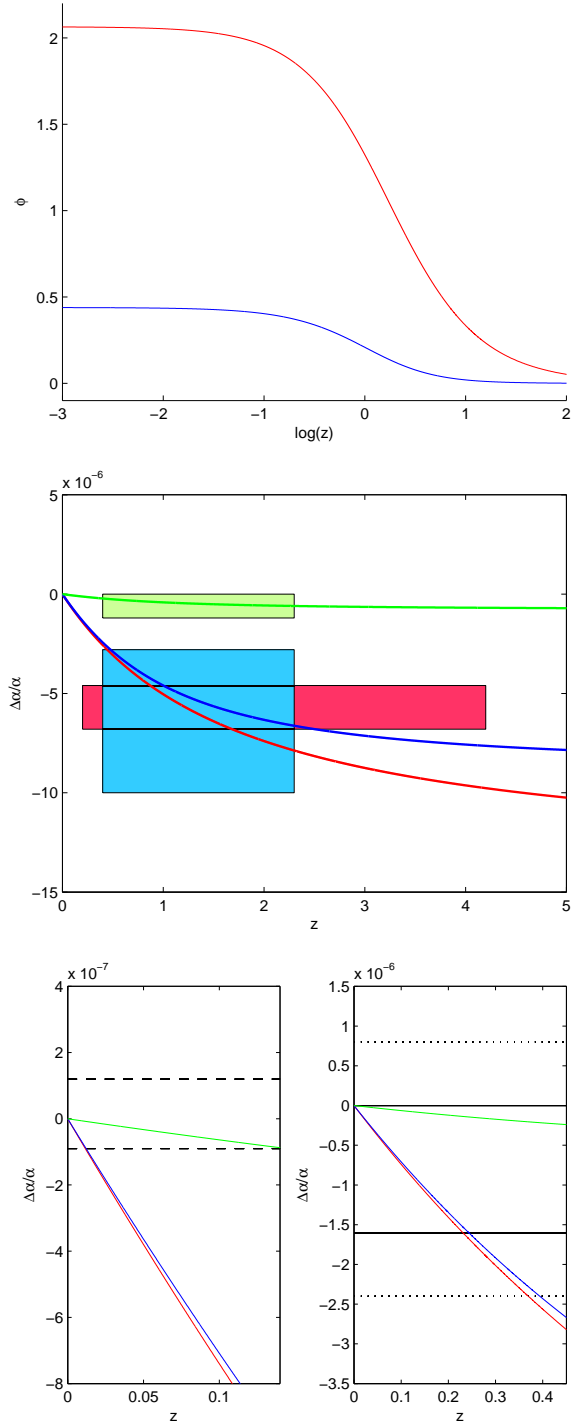


FIG. 8: *Top panel:* The evolution of the scalar field ϕ under the potential I with respect to redshift z , the red and blue curves are obtained by the best-fit values of KWM143 and VCS23 (VWM23) respectively. *Middle panel:* the evolution of $\Delta\alpha/\alpha$ with respect to z . The red, blue and green curves are obtained by the use of the best-fit values of KWM143, VWM23 and VCS23 respectively, while the boxes are the corresponding weighted values of QSO observations. *Bottom Left:* The comparison of the QSO results with Oklo bound (dashed lines); *Bottom Right:* The comparison with meteorite bound (the solid and dotted lines correspond to 1σ and 2σ , respectively).

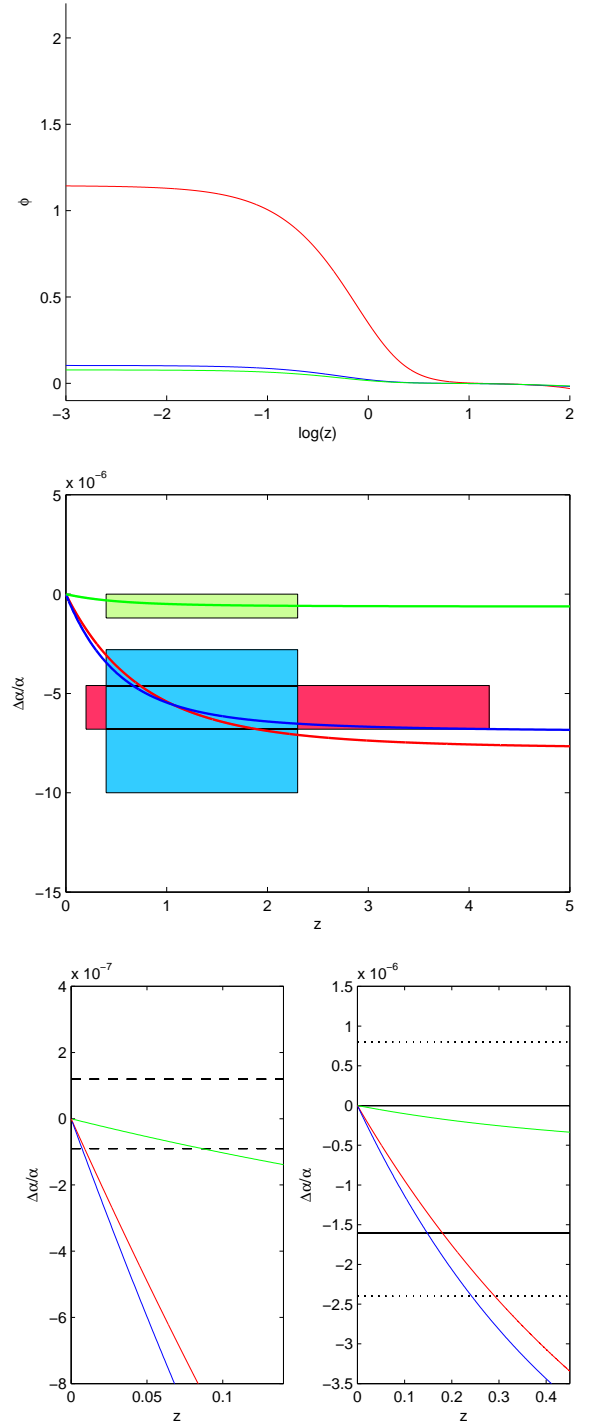


FIG. 9: The same as FIG.8 but for Model II.

Furthermore, we should point out that the observations of the variations of α by QSOs are not efficient as other cosmic probes. This feature is reflected in their insensitivity to the cosmological parameters such as n or λ , because the sufficient constraints of the confident regions are also necessary as the best-fit values. Except

that, further researches on the distribution or the precise value of ζ are important. And the comparisons between them with the QSO research are also imperative. If we hope to get more accurate description of $\Delta\alpha/\alpha$, measuring ζ accurately or combined with other observations will be necessary[52].

Note added, we notice that recently, the correlation of the cosmic dipoles between the fine structure constant and the supernovae are studied in Ref.[89]. From the theoretical view, exploring this correlation under the scalar field assumption and reconstruct the quintessence model is also worth studying. And we will discuss this question in our future research.

V. ACKNOWLEDGEMENT

We are very grateful to the anonymous referee for many valuable comments that greatly improved the pa-

per. The authors would like to thank Liu, W., Wang, H., Chen, Y., Landau, S. J., Meng, X. and Ma, C. for their helpful discussions and valuable suggestions. This research is supported by the National Science Foundation of China (Grant Nos. 11173006, 10773002, 10875012, 11175019), the Ministry of Science and Technology National Basic Science program (project 973) under grant No. 2012CB821804, and the Fundamental Research Funds for Central Universities.

-
- [1] Uzan, J.-P., Living Rev. Rel. 14, 2 (2011)
 - [2] Dirac, P. A. M., Nature(London) 139,323 (1937)
 - [3] Dirac, P. A. M., Proc. Roy. Soc. London A, 165,198 (1938)
 - [4] Barrow, J. D., Phil. Trans. Roy. Soc. Lond. A 363, 2139 (2005)
 - [5] Barrow, J. D., eprint, arXiv: 0912.5510 (2009)
 - [6] Chiba, T., eprint, arXiv: 1111.0092 (2011)
 - [7] Damour, T., Space Sci. Rev. 148, 191 (2009)
 - [8] Flambaum, V. V., Eur. Phys. J. ST, 163, 159 (2008)
 - [9] Garcia-Berro, E., Isern, J. and Kubyshev, Y. A., Astro. Astrophys. Rev. 14, 113 (2007)
 - [10] Karshenboim, S. G., Gen. Rel. Grav. 38, 159 (2006)
 - [11] Uzan, J.-P., Rev. Mod. Phys. 75, 403 (2003)
 - [12] Bekenstein, J. D., Phys.Rev.D, 25, 1527 (1982)
 - [13] Sandvik, H.B., Barrow, J.D., and Magueijo, J., Phys.Rev.Lett.88, 031302(2002); Phys.Rev.D 65, 063504(2002); Phys.Rev.D 65, 123501(2002); Phys.Rev.D 60, 043515(2002); Phys.Lett.B 541, 201(2002)
 - [14] Damour, T. and Dyson, F., Nucl. Phys. B, 480, 37 (1996)
 - [15] Olive, K. A. et.al, Phys. Rev. D, 66, 045022 (2002)
 - [16] Avelino, P. P. et al, Phys. Rev. D, 64, 103505 (2001)
 - [17] Martins, C. J. A. et al, Phys. Lett. B, 585, 29 (2004)
 - [18] Nollett, K. M. and Lopez, R. E., Phys. Rev. D, 66, 063507 (2002)
 - [19] Landau, S. J. and Scóccola, C. G., eprint, arXiv: 1002.1603 (2010)
 - [20] Menegoni, E. et al., Phys. Rev. D, 80, 087302 (2009)
 - [21] Nakashima, M., Nagata, R. and Yokoyama, J.,Prog. Theor. Phys., 120 , 1207 (2008)
 - [22] Chand, H. et al, Astron. Astrophys. 417, 853 (2004)
 - [23] Murphy, M. T. et al, Mon. Not. Roy. Astron. Soc., 327, 1208 (2001a); Mon. Not. Roy. Astron. Soc., 327, 1237 (2001b); Mon. Not. Roy. Astron. Soc., 327, 1244 (2001c); Mon. Not. Roy. Astron. Soc., 345, 609 (2003); Lect. Notes Phys. 648, 131 (2004).
 - [24] Sriannand, R. et al, Phys. Rev. Lett., 92, 121302 (2004)
 - [25] Webb, J. K. et al, Phys. Rev. Lett. 82, 884 (1999); Phys. Rev. Lett. 87, 091301 (2001); Astrophys. Space Sci. 283, 565 (2003)
 - [26] Landau, S. J. and Simeone, C., Astron. Astrophys., 487, 857 (2008)
 - [27] Eisenstein, D. J. et al., Astrophys.J. 633, 560 (2005)
 - [28] Hicken, M. et al., Astrophys.J., 700, 1097 (2009)
 - [29] Komatsu, E. et al., Astrophys. J. Suppl. 192, 18 (2011)
 - [30] Percival, W. J. et al., Mon.Not.Roy.Astron.Soc. 401, 2148 (2010)
 - [31] Riess, A. G. et al., Astrophys.J. 116, 1009 (1998)
 - [32] Spergel, D. N. et al., Astrophys.J.S. 170, 377 (2007)
 - [33] Tsujikawa, S., eprint, arXiv: 1004.1493 (2010); Int. J. Mod. Phys. D, 15, 1753 (2006)
 - [34] Chen, Y. and Ratra, B., Phys. Lett. B, 703, 406 (2011)
 - [35] Li, M. et al, Commun. Theor. Phys., 56, 525 (2011)
 - [36] Samushia, L., PhD thesis, eprint, arXiv: 0908.4597; Samushia, L. and Ratra, B., Astrophys. J., 650, L5 (2006); Samushia, L. and Ratra, B., Astrophys. J., 701, 1373 (2009) and references therein.
 - [37] Ma, C. and Zhang, T., Astrophys, J. 730, 74 (2011)
 - [38] Moresco, M. et al., eprint: arXiv: 1201.6658
 - [39] Zhang, T., Ma, C. and Lan, T., Advances in Astronomy, 184284 (2010)
 - [40] Peebles, P. J. E. and Ratra, B., Astrophys. J., 325, L17 (1988)
 - [41] Ratra, B. and Peebles, P. J. E., Phys. Rev. D 37, 3406 (1988)
 - [42] Watson, C. R. and Scherrer, R. J., Phys. Rev. D., 68, 123524 (2003)
 - [43] Steinhardt, P. J., Wang, L. M. and Zlatev, I., Phys. Rev. D, 59, 123504 (1999)
 - [44] Zlatev, I., Wang, L. M. and Steinhardt, P. J., Phys. Rev. Lett. 82, 896 (1999)
 - [45] Wetterich, C., Nucl. Phys. B, 302, 668 (1988)
 - [46] Doran, M. and Wetterich, C., eprint, arXiv: astro-ph/0205267
 - [47] Bozek, B. et al., Phys. Rev. D, 77, 103504 (2008)

- [48] Wang, P., Chen, C. and Chen, P., eprint, arXiv: 1108.1424
- [49] Avilino, P. P. et al, Phys. Rev. D, 74, 083508 (2006)
- [50] Nunes, N. J. and Lidsey, J. E., Phys. Rev. D, 69, 123511 (2004); eprint: arXiv: 0910.4935
- [51] Parkinson, D., Bassett, B. A. and Barrow, J. D., Phys. Lett. B, 578, 235 (2004)
- [52] Amendola, L. et al, eprint: arXiv: 1109.6793
- [53] Russo, J. G., Phys. Lett. B, 600, 185 (2004)
- [54] Binetruy, P., Int. J. Theor. Phys., 39, 1859 (2000)
- [55] Binetruy, P., Phys. Rev. D, 60, 063502
- [56] Ferreira, P. G. and Joyce, M., Phys. Rev. D, 58, 023503
- [57] Copeland, E. J., Nunes, N. J. and Pospelov, M., Phys. Rev. D, 69, 023501 (2004)
- [58] Marra, V. and Rosati, F., J.C.A.P., 0505, 011 (2005)
- [59] Dzuba, V. A., Flambaum, V. V. and Webb, J. K., Phys. Rev. Lett., 82, 888 (1999)
- [60] Murphy, M. T. et al, Phys. Rev. Lett., 99, 239001 (2007); Mon. Not. Roy. Astron. Soc., 384, 1053 (2008);
- [61] King, J. A. et al., eprint, arXiv: 1202.4758
- [62] Barrow, J. D. and Li, B., Phys. Rev. D, 78, 083536 (2008)
- [63] Bento, M. C. and Felipe, R. G., Phys. Lett. B, 674, 146 (2009)
- [64] Bisabr, Y., Phys. Lett. B, 688, 4 (2010)
- [65] Calabrese, E. et al., Phys. Rev. D, 84, 023518 (2011)
- [66] Fujii, Y., Phys. Lett. B, 671, 207 (2009)
- [67] Gutiérrez, C. M. and López-Corredoira, M., Astrophys.J., 713, 46 (2010)
- [68] Lee, S., Olive, K. A. and Pospelov, M., Phys. Rev. D, 70,083503 (2004);
- [69] Mosquera, M. E. et al., Astron. Astrophys., 478, 675 (2008)
- [70] Tedesco, L., eprint, arXiv: 1106.3436 (2011)
- [71] Toms, D. J., Phys. Rev. Lett., 101, 131301 (2008)
- [72] Avelino, P. P. et al., eprint, arXiv: 1112.3878
- [73] Farajollahi, H. and Salehi, A., J. C. A. P., 02, 042 (2012)
- [74] Martinelli, M., Menegoni, E. and Melchiorri, A., eprint, arXiv: 1202.4373
- [75] Thompson, R. I., eprint, arXiv: 1202.3977
- [76] Berengut, J. C. et al., Phys. Rev. D, 83, 123506 (2011)
- [77] Berengut, J. C. et al., eprint, arXiv: 1203.5891
- [78] Webb, J. K. et al., Phys. Rev. Lett., 107, 191101 (2011)
- [79] Copeland, E. J., Sami, M. and Tsujikawa, S., Int. J. Mod. Phys. D, 15, 1753 (2006)
- [80] Olive, K. A. and Pospelov, M., Phys. Rev. D, 65, 085044 (2002)
- [81] Avelino, P. P. et al, Phys. Rev. D, 70, 083506 (2004); Avelino, P. P. et al, J. C. A. P., 0612, 018 (2006)
- [82] Damour, T., eprint: arXiv: gr-qc/0306023
- [83] Will, C. M., Living Rev. Rel. 4, 4 (2001)
- [84] Fujii, Y., Nucl. Phys. B, 573, 377 (2000)
- [85] Fujii, Y., Phys. Lett. B, 573, 39 (2003)
- [86] Olive, K. A. et al., Phys. Rev. D, 69, 027701 (2004)
- [87] Fujii, y. and Iwamoto, A., Phys. Rev. Lett., 91, 261101 (2003)
- [88] Bento, M. C., Bertolami, O. and Santos, N. M. C., Phys. Rev. D, 70, 107304 (2004)
- [89] Mariano, A. and Perivolaropoulos, L., eprint, arXiv: 1206.4055

0.22909	2.549	5.395	KWM143
0.5194	-3.365	3.256	KWM143
0.5533	-1.837	1.716	KWM143
0.58596	-1.977	4.53	KWM143
0.59137	-3.105	2.433	KWM143
0.61256	0.372	1.191	KWM143
0.633	4.282	4.088	KWM143
0.65741	7.123	4.608	KWM143
0.6596	0.444	1.505	KWM143
0.6681	0.075	1.475	KWM143
0.69404	-1.92	3.916	KWM143
0.72508	-2.634	3.523	KWM143
0.729	0.041	1.297	KWM143
0.73117	-1.211	0.976	KWM143
0.7455	-2.056	0.745	KWM143
0.773	2.228	1.179	KWM143
0.79026	0.088	0.59	KWM143
0.80757	1.215	1.221	KWM143
0.84142	0.579	0.804	KWM143
0.8431	0.102	0.846	KWM143
0.85048	-6.9	7.023	KWM143
0.85118	0.475	1.022	KWM143
0.8514	-0.34	1.284	KWM143
0.8545	-0.021	1.27	KWM143
0.859	0.578	1.205	KWM143
0.86182	-2.024	1.636	KWM143
0.9029	-0.999	1.783	KWM143
0.9108	-0.391	0.609	KWM143
0.92741	-0.28	0.777	KWM143
0.9277	-0.218	1.39	KWM143
0.9341	1.877	1.796	KWM143
0.94398	0.758	2.337	KWM143
0.948	-3.664	1.857	KWM143
0.9901	-2.202	1.293	KWM143
0.9902	1.156	2.399	KWM143
1.0092	-0.193	1.009	KWM143
1.0158	-2.098	0.937	KWM143
1.017	-0.318	0.734	KWM143
1.0172	1.044	0.865	KWM143
1.0465	-0.75	1.514	KWM143
1.0479	-0.202	2.199	KWM143
1.0598	-0.751	1.643	KWM143
1.0981	-3.57	1.22	KWM143
1.1117	-5.459	2.508	KWM143
1.1161	0.005	1.964	KWM143
1.1314	0.561	0.789	KWM143
1.1425	-0.092	0.663	KWM143
1.1534	-0.743	1.787	KWM143
1.1726	-3.204	1.546	KWM143
1.1745	-3.033	1.093	KWM143
1.2128	1.326	1.49	KWM143
1.2189	-0.521	0.542	KWM143
1.2259	0.28	1.433	KWM143
1.2294	-1.472	0.818	KWM143
1.2324	0.981	2.757	KWM143
1.2667	-1.268	1.462	KWM143
1.2679	2.057	2.521	KWM143
1.2938	-1.393	0.624	KWM143
1.3192	-2.587	2.41	KWM143
1.3196	-0.725	0.761	KWM143
1.325	0.703	0.804	KWM143
1.3422	-0.853	1.169	KWM143
1.3428	-1.29	0.949	KWM143

TABLE I: Direct measurements of the observational variation of the fine structure constant

z_{abs}	$\Delta\alpha/\alpha(10^{-5})$	1σ uncertainty(10^{-5})	data sample
-----------	--------------------------------	------------------------------------	-------------

1.365	-0.222	0.523	KWM143	2.8114	0.919	1.954	KWM143
1.4162	-0.904	0.56	KWM143	2.8268	0.319	0.929	KWM143
1.4342	-1.253	1.167	KWM143	2.8433	-4.959	1.334	KWM143
1.476	-0.658	1.216	KWM143	2.8677	-1.878	3.977	KWM143
1.5337	-1.345	1.156	KWM143	2.9587	1.861	2.621	KWM143
1.5541	-1.87	0.878	KWM143	3.0173	0.822	2.196	KWM143
1.5899	0.449	1.163	KWM143	3.0173	1.226	3.289	KWM143
1.6111	-2.489	2.022	KWM143	3.025	-2.835	3.422	KWM143
1.6112	-1.298	1.727	KWM143	3.1513	-4.111	3.441	KWM143
1.7385	-0.194	1.861	KWM143	3.2351	0.855	1.824	KWM143
1.7549	-1.465	2.178	KWM143	3.2534	-2.494	3.532	KWM143
1.768	0.046	1.235	KWM143	3.3172	2.747	6.067	KWM143
1.794	-1.295	1.05	KWM143	3.3897	-7.843	3.548	KWM143
1.7954	0.648	1.415	KWM143	3.439	0.937	3.912	KWM143
1.8024	-2.001	1.267	KWM143	3.6061	-0.42	4.402	KWM143
1.858	-5.48	2.11	KWM143	3.6663	-0.599	3.503	KWM143
1.864	-1.012	1.821	KWM143	4.1798	1.237	3.933	KWM143
1.8918	-0.445	1.972	KWM143	0.452	0.200	0.500	VCS23
1.92	1.399	1.889	KWM143	0.822	0.000	0.900	VCS23
1.956	1.992	2.043	KWM143	0.859	-0.300	0.200	VCS23
1.9746	0.286	2.326	KWM143	0.873	0.000	0.200	VCS23
1.99	-1.562	1.971	KWM143	0.908	-0.400	0.400	VCS23
1.999	5.498	3.63	KWM143	0.943	-1.20	0.700	VCS23
2.0653	1.717	2.153	KWM143	1.183	0.000	0.800	VCS23
2.066	-2.614	2.027	KWM143	1.243	-0.100	0.100	VCS23
2.0762	1.526	3.722	KWM143	1.277	-0.100	0.200	VCS23
2.095	0.034	1.898	KWM143	1.349	-0.600	0.400	VCS23
2.0994	-0.813	2.621	KWM143	1.439	0.000	0.500	VCS23
2.1053	4.361	3.976	KWM143	1.542	0.000	0.200	VCS23
2.1102	-0.164	1.168	KWM143	1.556	0.200	0.500	VCS23
2.14	-5.418	2.782	KWM143	1.636	0.200	0.700	VCS23
2.1406	-0.865	1.956	KWM143	1.637	0.600	0.600	VCS23
2.154	3.605	3.954	KWM143	1.657	0.300	0.500	VCS23
2.1711	-0.944	1.204	KWM143	1.858	0.400	0.400	VCS23
2.279	1.366	4.161	KWM143	1.915	0.800	0.300	VCS23
2.309	-3.949	2.225	KWM143	2.023	-0.100	0.400	VCS23
2.3103	-2.245	6.439	KWM143	2.168	0.000	0.400	VCS23
2.325	0.017	1.64	KWM143	2.185	0.200	0.300	VCS23
2.3742	1.411	2.105	KWM143	2.187	-0.200	0.200	VCS23
2.375	2.265	4.21	KWM143	2.301	-0.400	0.400	VCS23
2.4264	-4.879	3.485	KWM143	0.452	-0.963	1.6847	VWM23
2.43	-1.322	1.794	KWM143	0.822	1.062	1.7372	VWM23
2.4389	-0.939	1.712	KWM143	0.859	-4.803	1.7792	VWM23
2.457	-5.853	2.597	KWM143	0.873	-0.100	1.6129	VWM23
2.462	0.576	2.463	KWM143	0.908	-1.507	1.6067	VWM23
2.4653	-1.306	2.412	KWM143	0.943	-1.453	1.7338	VWM23
2.4653	1.654	1.908	KWM143	1.183	0.249	1.6923	VWM23
2.4673	6.973	4.395	KWM143	1.243	-2.447	2.1848	VWM23
2.476	-4.664	2.64	KWM143	1.277	0.524	2.5558	VWM23
2.5378	-3.856	2.277	KWM143	1.349	-2.724	1.8944	VWM23
2.548	1.015	6.186	KWM143	1.439	-1.272	1.6936	VWM23
2.5548	-1.851	6.572	KWM143	1.542	-4.655	1.8045	VWM23
2.5577	-0.253	3.503	KWM143	1.556	0.183	1.6396	VWM23
2.5577	0.419	1.198	KWM143	1.636	-0.124	1.5900	VWM23
2.6021	-1.629	2.272	KWM143	1.637	1.539	1.7782	VWM23
2.6147	-0.697	4.186	KWM143	1.657	0.510	1.5951	VWM23
2.6238	2.141	7.358	KWM143	1.858	0.315	1.6694	VWM23
2.625	-0.591	2.494	KWM143	1.915	0.767	1.6350	VWM23
2.625	-0.751	2.236	KWM143	2.023	-2.725	2.0215	VWM23
2.6532	-3.31	2.614	KWM143	2.168	0.115	1.6776	VWM23
2.7504	2.485	4.788	KWM143	2.185	3.926	2.8618	VWM23
2.7698	-0.688	1.866	KWM143	2.187	-0.122	1.6968	VWM23
2.7955	4.109	9.498	KWM143	2.301	-0.075	1.8117	VWM23

